Model of joint displacement using sigmoid function. Experimental approach for planar pointing task and squat jump

T. Creveaux*, J. Bastien, C. Villars and P. Legreneur

**Université de Lyon, CRIS, 27-29 Bd du 11 Novembre 1918, 69622 Villeurbanne Cedex, France. thomas.creveaux@univ-lyon1.fr*

Abstract. Using an experimental optimization approach, this study investigated whether two human movements, pointing tasks and squat-jumps, could be modeled with a reduced set of kinematic parameters. Three sigmoid models were proposed to model the evolution of joint angles. The models parameters were optimized to fit the 2D position of the joints obtained from pointing tasks and 120 squat-jumps. The models were accurate for both movements. This study provides a new framework to model planar movements with a small number of meaningful kinematic parameters, allowing a continuous description of both kinematics and kinetics. Further researches should investigate the implication of the control parameters in relation to motor control and validate this approach for three-dimensional movements.

1. Introduction

Quantitative analysis of human movement usually relies on the time history of reflective markers fixed to anatomical landmarks obtained from optical systems. These raw data are further used to compute relevant parameters such as velocities, accelerations, moments or powers. During the recent years, the performance of acquisition systems greatly increased, especially considering acquisition rate and accuracy. However, raw data still remain noisy, due to the movement of the skin with regard to the bones and finite accuracy of such systems. Furthermore, the effect of noise increases as the data is derived with respect to time, which is a very common task in movement analysis.

To overcome the above issues, raw data are quite always smoothed or filtered, resulting in well-known decrease of movement amplitude. Specific filtering methods accounting for properties of the skeletal system such as constant length of the limbs have been used but such approaches still suffer from the motion of the markers relatively to the skeletal system. An interesting feature of human motion is the necessity for decelerating the joint displacement before its maximal amplitude (anatomical constraint) in order to protect this joint from any damage (van Ingen Schenau, 1989). Regarding to kinematics, the anatomical constraint implies that joint angular time history should match an asymmetric sigmoid shape (Zelaznik et al., 1986) and thus an asymmetric bell-shaped velocity profile (Soechting and Lacquaniti, 1981), which accounts for synergistic actuators' activations at a joint, i.e. agonist and antagonist muscle-tendon systems. In the field of human movement analysis, Plamondon proposed a model of asymmetric sigmoid (Plamondon, 1995, 1998; Plamondon et al., 2003). However, the velocity is not null at the end of the movement so that the anatomical constraint is not satisfied.

Therefore, this study aimed at modeling two different movements, i.e. a pointing task and an explosive movement, the squat-jump, using a generic model of sigmoidal joint displacement based on meaningful kinematic parameters which accounts for the anatomical constraint. Three sub models were used to achieve best fitting of experimental data obtained from both movements (Creveaux et al., 2012).

2. Methods

2.1 General model of joint displacement

Accounting for a monotone evolution of a given angle and considering the anatomical constraint requirements, it is assumed that each angle θ is characterized by the following properties (figure 1):

- at the beginning and at the end of the movement, the velocity and the acceleration are equal to zero;
- the angle increases (respectively decreases) throughout the whole movement;
- during the movement, the velocity increases (respectively decreases) until it reaches its maximum (respectively minimum), then decreases (respectively increases).

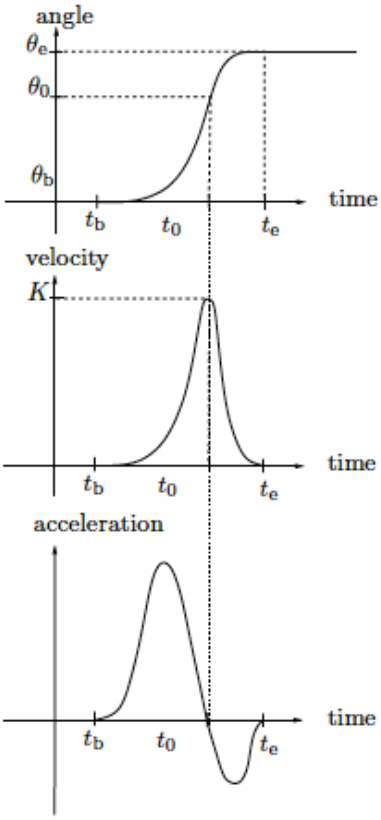

Figure 1. Shape of used sigmoid: angle, velocity and acceleration versus time (for the increasing case).

More precisely, we try to determine a function θ from $[0,T]$ to $\mathbb{R}$ of class C^2. Let t_b, t_0, t_e be three instants such that

$$0 \leq t_b < t_0 < t_c \leq T \tag{2.1}$$

Let θ_b, θ_0, θ_e be three real numbers such that

$$\theta_b < \theta_0 < \theta_e \text{ or } \theta_e < \theta_0 < \theta_b \tag{2.2}$$

We assume that

- θ is constant and equals to θ_b on $[0, t_b]$;
- θ is constant and equals to θ_e on $[t_e, T]$;
- there exists $\varepsilon \in \{-1,1\}$ such that $\varepsilon\theta$ is strictly increasing on $[t_b, t_e]$;
- $\varepsilon\theta$ is strictly convex on (t_b, t_0);
- $\varepsilon\theta$ is strictly concave on (t_0, t_e);

We set

$$\varepsilon = Sign(\theta_e - \theta_b) \epsilon \{-1,1\} \tag{2.3}$$

Let K be the number defined by

$$K = \begin{cases} max\ \theta'(t), t \in [t_b, t_e] & if\ \varepsilon = 1 \\ min\ \theta'(t), t \in [t_b, t_e] & if\ \varepsilon = -1 \end{cases} \tag{2.4}$$

Since θ is of class C^2, we have

$$\theta(t_b) = \theta_b, \quad \theta'(t_b) = 0, \quad \theta"(t_b) = 0 \tag{2.5a}$$
$$\theta(t_e) = \theta_b, \quad \theta'(t_e) = 0, \quad \theta"(t_e) = 0 \tag{2.5b}$$
$$\theta(t_0) = \theta_b, \quad \theta'(t_0) = 0, \quad \theta"(t_0) = 0 \tag{2.5c}$$
$$\forall t \in (t_b, t_0), \quad \varepsilon\theta"(t) > 0 \tag{2.5d}$$
$$\forall t \in (t_0, t_e), \quad \varepsilon\theta"(t) < 0 \tag{2.5e}$$

We consider α, $\beta \in (0,1)$ and $k \in \mathbb{R}$ defined by

$$\alpha = \frac{t_0 - t_b}{t_e - t_b} \quad \beta = \frac{\theta_0 - \theta_b}{\theta_e - \theta_b} \quad k = K\frac{t_e - t_b}{\theta_e - t_b} \tag{2.6}$$

Applying the following change of scale,

$$\forall t \in [t_b, t_e], \quad u = \frac{t - t_b}{t_e - t_b} \in [0,1] \tag{2.7a}$$

$$\forall u \in [0,1], \quad g(u) = \frac{\theta\big((t_e - t_b)u + t_b\big) - \theta_b}{\theta_e - \theta_b} \tag{2.7b}$$

The problem can be reformulated as follow: we search a function g of class C^2 defined on $[0,1]$ satisfying:

$$g(0) = 0, \quad g'(0) = 0, \quad g"(0) = 0 \tag{2.8a}$$
$$g(1) = 1, \quad g'(1) = 0, \quad g"(1) = 0 \tag{2.8b}$$
$$g(\alpha) = \beta, \quad g'(\alpha) = k, \quad g"(\alpha) = 0 \tag{2.8c}$$
$$\forall u \in (0,\alpha), \quad g"(t) > 0 \tag{2.8d}$$
$$\forall u \in (\alpha,1), \quad g"(t) < 0 \tag{2.8e}$$

Remark 2.1. Under the assumptions given in (2.8), we have necessarily

$$k \geq max\left(\frac{\beta}{\alpha}, \frac{1-\beta}{1-\alpha}\right) > 1 \tag{2.9}$$

Finally, the function θ is defined for all $t \in [0,T]$ by

$$\theta(t) = \begin{cases} \theta_b, & if\ t \leq t_b \\ (\theta_e - \theta_b) g\left(\dfrac{t - t_b}{t_e - t_b}\right) + \theta_b, & if\ t_b < t < t_e \\ \theta_e, & if\ t \geq t_e \end{cases} \tag{2.10}$$

This function if defined by 7 independent parameters:

- 2 time scale parameters (t_b and t_e);
- 2 angle scale parameters (θ_b and θ_e);
- 3 shape parameters (α, β, k).

Thus, θ can be written under the form $\theta_{t_b,t_e,\theta_b,\theta_e,\alpha,\beta,k}$. Aimed to solve the system (2.8), we have to include into the model 3 control parameters, which have to be related with α, β and k. In the next section, 3 sigmoid models, *i.e.* SYM, NORM and INVEXP are presented.

2.2 The SYM model

The SYM model was built using a pseudo-symmetry approach. Its function g is defined by $\alpha, \beta \in (0,1)$ and $\kappa > 1$. Let $g_{\alpha,\beta,k}$ be a function of class C^2 from $[0,\alpha]$ to $\mathbb{R}$ satisfying (2.8a), (2.8c) and (2.8d). If the function g is defined from $[0,1]$ to $\mathbb{R}$ by,

$$g(u) = \begin{cases} g_{\alpha,\beta,k}(u), & if\ u \leq \alpha \\ 1 - g_{1-\alpha,1-\beta,k}(1-u), & if\ u > \alpha \end{cases} \tag{2.11}$$

Then, g is of class C^2 on $[0,1]$ and (2.8) holds. Considering the function $H_{a,b,\kappa}$ defined on $[0,\alpha]$ for all $a, b > 0$ and $\kappa > 2$ as

$$H_{a,b,\kappa}(u) = a\big(1 - e^{-bu^\kappa}\big) \tag{2.12}$$

a, b and κ have to be determined so that (2.8a), (2.8c) and (2.8d) hold. We set

$$r_0 = \frac{1}{e^{0.5} - 1} \approx 1.54 \tag{2.13}$$

For all $(\alpha, \beta) \in (0,1)^2$, for all k such that $k > r_0\,\beta/\alpha$, there exists $(a, b, \kappa) \in {\mathbb{R}_+^*}^2 \times (2, \infty)$ such that (2.8a), (2.8c) and (2.8d) hold for function $H_{a,b,\kappa}$. a, b and κ still need to be defined. We set

$$\gamma = \frac{\beta}{k\alpha} \in (0, e^{0.5} - 1) \tag{2.14a}$$

It exists an unique $X \in (0.5,1)$ such that

$$(e^X - 1)\frac{1 - X}{X} = \gamma \tag{2.14b}$$

It follows

$$a = \frac{\beta}{1 - e^{-X}} \quad b = \frac{X}{\alpha^\kappa} \quad \kappa = \frac{1}{1 - X} \tag{2.14c}$$

By setting $(a, b, \kappa) = G(\alpha, \beta, k)$, the function g is defined for all $u \in [0,1]$ by

$$g(u) = \begin{cases} H_{G(\alpha,\beta,k)}(u), & if\ u \leq \alpha \\ 1 - H_{G(1-\alpha,1-\beta,k)}(1-u), & if\ u > \alpha \end{cases} \tag{2.15}$$

2.3 The NORM model

The NORM model (named from its relation to the normal law) function g is defined by 3 parameters $a \in (0,1)$, $p > 0$ and $s > 0$. As a reminder, the density function of the normal, or Gaussian distribution with mean m and variance s^2 is given by:

$$\forall x \in \mathbb{R}, f(x) = \frac{1}{s\sqrt{2\pi}} exp\left(-\frac{1}{2}\left(\frac{x-m}{s}\right)^2\right) \tag{2.16}$$

Considering the erf function defined by

$$\forall x \in \mathbb{R}, \text{erf}(t) = \frac{2}{\pi}\int_0^x e^{-t^2} dt \tag{2.17}$$

The cumulative distribution function of the normal law is given by

$$\forall x \in \mathbb{R}, \Phi(x) = \frac{1}{2} erf\left(\frac{x-m}{\sqrt{2s}}\right) + \frac{1}{2} \tag{2.18}$$

For all $p > 0$

$$\forall u \in (0,1), \mathrm{G}(u) = ln\left(\frac{u^p}{1-u^p}\right) \tag{2.19}$$

The function g is defined by

$$\forall t \in (0,1), \quad g(t) = \Phi\big(G(t)\big) \tag{2.20a}$$

$$g(0) = 0 \tag{2.20b}$$

$$g(1) = 1 \tag{2.20c}$$

2.4 The INVEXP model

The INVEXP model (derived from the inverse exponential) function g is defined by 3 parameters $\lambda, \mu > 0$ and $a \in \mathbb{R}$. For all a, for all λ and μ we set

$$\alpha = \frac{\lambda}{\lambda + \mu} \in (0,1) \tag{2.21}$$

and we consider the function $g_{a,\alpha}$ as:

$$g_{a,\alpha} = 1, \qquad if\ a = 0 \tag{2.22a}$$

$$\begin{cases} \forall y \in [0, \alpha[& g_{a,\alpha}(y) = 1 - exp\left(\dfrac{t}{a(t-\alpha)}\right) \\ \forall y \in [\alpha, 1] & g_{a,\alpha}(y) = 1 \end{cases} \qquad if\ a > 0 \tag{2.22b}$$

For all $a \in \mathbb{R}$ and for all $\alpha \in (0,1)$, we consider the function $G_{a,\alpha}$ defined by

$$\begin{cases} if\ a \geq 0, & G_{a,\alpha} = g_{a,\alpha} \\ if\ a < 0, & G_{a,\alpha} = g_{-a,1-\alpha} \end{cases} \tag{2.23}$$

For all $\lambda, \mu > 0$, $f_{\lambda,\mu}$ is defined by

$$\forall t \in (0,1), \quad f_{\lambda,\mu}(t) = exp\left(-\frac{1}{t^\lambda (1-t)^\mu}\right) \tag{2.24a}$$

$$f_{\lambda,\mu}(0) = 0 \tag{2.24b}$$

$$f_{\lambda,\mu}(1) = 1 \tag{2.24c}$$

For all $a \in \mathbb{R}$, $\lambda, \mu > 0$, $h_{\lambda,\mu,a}$ is defined by:

$$h_{\lambda,\mu,a} = f_{\lambda,\mu} G_{a,\lambda/(\lambda+\mu)} \tag{2.25}$$

The function g is defined by

$$\forall t \in (0,1), \quad g(t) = \frac{\int_0^t h_{\lambda,\mu,a}(u)du}{\int_0^1 h_{\lambda,\mu,a}(u)du} \tag{2.26}$$

2.5 Definition domains of the sigmoid models

Each of the 3 functions is defined by 3 parameters. For all $k > 1$, there exist a part S_k of $(0,1)^2$ such that for all $(\alpha, \beta) \in S_k$, there exist at least one sigmoid of kind g satisfying (2.8) whose parameters can be determined by splitting (2.8) in 3 non-linear equations which can be solved with a numerical solver. This part S_k differs for the 3 sigmoid models. The bigger is obtained with the INVEXP model (Figure 2).

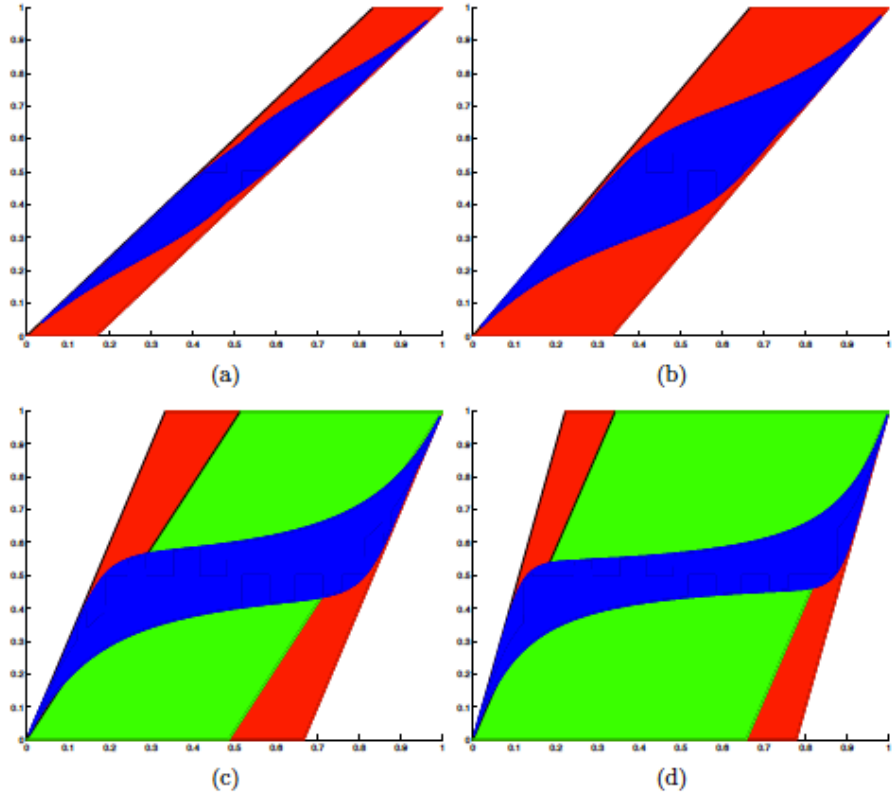

Figure 2. S_k domains of the three sigmoids for k=1.2 (a), k=1.5 (b), k=3 (c), and k=4.5 (d). INVEXP, NORM and SYM domains are plotted in red, blue and green respectively. According to (2.28), SYM domain is empty for k=1.2 and k=1.5.

Examples of position and velocity curves obtained from the three models are provided in figure 3.

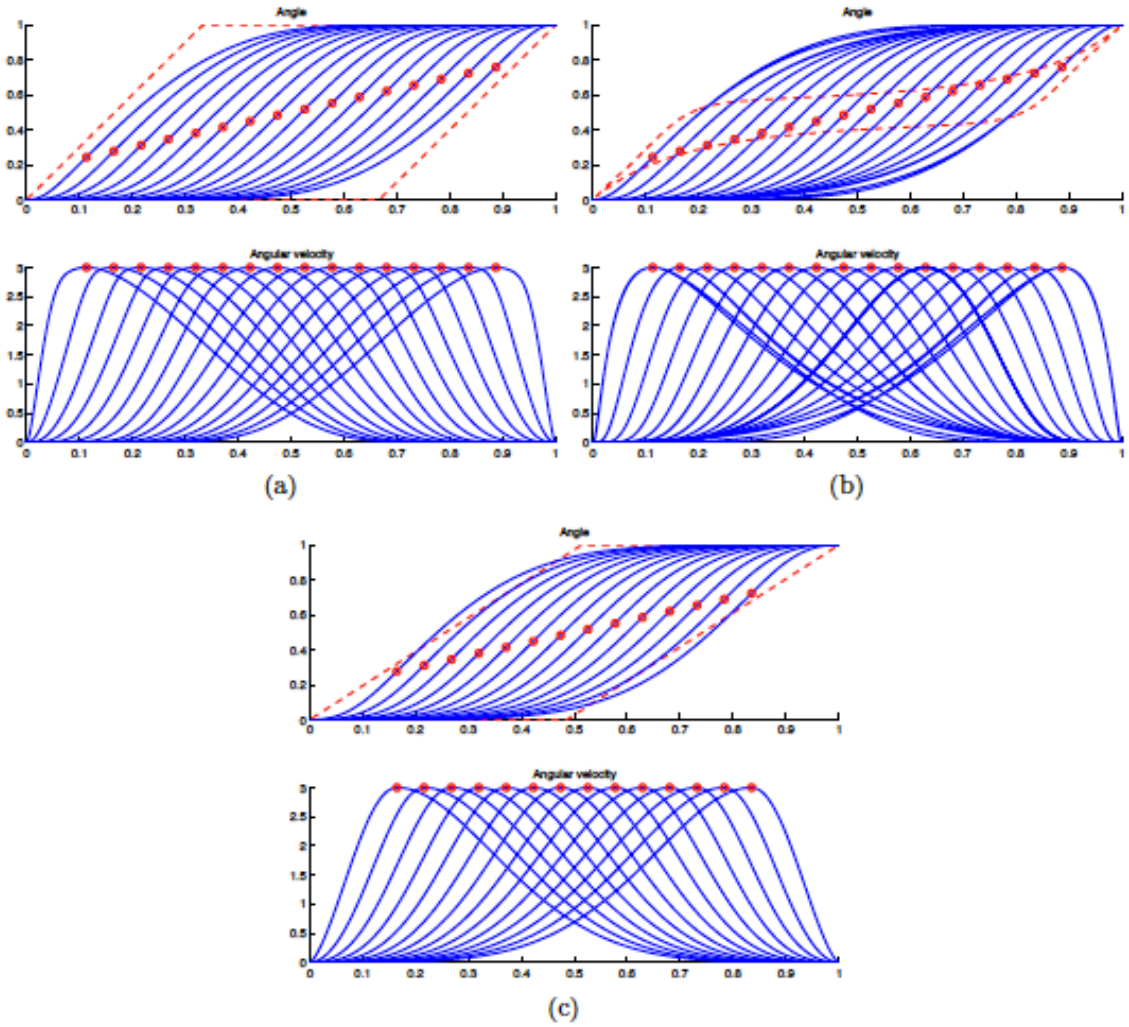

Figure 3. Examples of curves for angle and angular velocity for INVEXP (a), NORM (b) and SYM (c) models. The boundaries of domains are plotted in red dashed lines.

3. Experimental procedures

3.1 Pointing task

9 right-handed male subjects (age = 24.9 ± 2.42 years, height = 177.6 ± 5.83 cm and mass = 68.8 ± 8.18 kg) were asked to perform pointing tasks in the horizontal plane. The total number of pointing tasks was 304. Movements were performed for five directions and two distances (Figure 4). For each direction, two spherical targets were placed on a table at 60 and 80 cm from the shoulder. Directions of pointing task ranged regularly from 30 to 150 degrees including pointing along the antero-posterior axis. The described position of the targets ensures that each of them is located inside the subjects workspace (Figure 5) when considering a 80 cm upper limb length and the corresponding anthropometric dataset (Bastien et al., 2010). At the beginning of the movement, subjects had to position their arm so that the forefinger was located at 40 cm of the soulder in the antero-posterior direction. During the experiment, subjects sat on a chair whose height was adjusted so that the upper limb remained in the horizontal plane while moving over the table from starting point to targets and the trunk was immobilized by using straps. In order to ensure that the upper limb remained in the horizontal plane, the subjects were instructed to keep the upper limb lying on the table during the movements. Video reflective markers were placed on the subjects at the shoulder (acromion), elbow (olecrane), wrist (middle of radial and ulnar styloid processes) and forefinger extremity to allow further modeling of the upper limb. For each target, subjects performed three movements which were filmed at 25 Hz with a numeric camera JVC © Everio placed above the subjects and oriented vertically. Raw experimental data, *i.e.* the position of the joints throughout the movement, were extracted from videographic recordings.

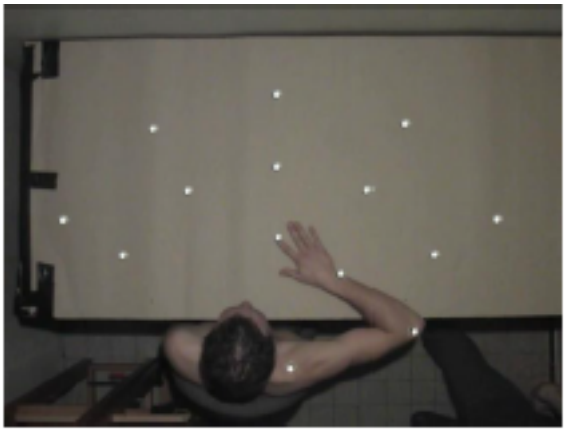

(a) Upper view of the task environment

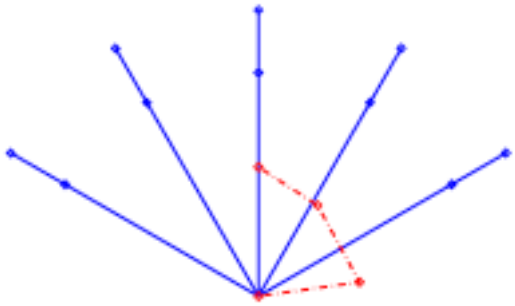

(b) Targets (continuous lines) and initial arm position (dashed line)

Figure 4. Pointing task experimental procedure.

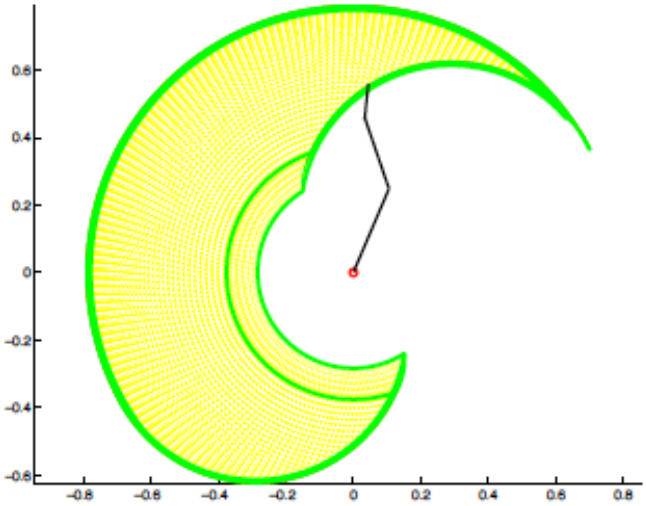

Figure 5. Upper limb workspace (adapted from (Bastien et al., 2010)).

3.2 Squat jumping

13 subjects performed 10 vertical jumps. Instructions were given for keeping the hands on the hips during the movement to limit the contribution of the upper limbs to the performance. Furthermore, subjects were asked to do no countermovement. The jumps that did not meet both of these requirements were excluded from the study. In order to model the skeleton in a 4 rigid segments system, landmarks were placed on the left fifth metatarsophalangeal, lateral malleolus, lateral femoral epicondyle, greater trochanter and acromion. These landmarks define the foot, the shank, the thigh and the upper body (Head, Arms and Trunk: HAT). The subjects were filmed orthogonally to the sagittal plane at 100 Hz and the ground reaction force was recorded at 1000 Hz from an OR6-7-2000 AMTI force plate. The center of mass (CoM) position of limbs was computed using anthropometric data (Winter, 2009). The whole body CoM (Center of Mass) position was determined on the one hand from kinematic data and on the other hand from force plate measurements using a double numerical integration procedure. For the latter, subject mass, initial body CoM position and velocity had to be set. These values were computed so that the difference between CoM path obtained from kinetic and kinematic data was minimized in a least square sense. This optimization step was also used to synchronize both recording sources.

4. Data processing

4.1 Skeletal model

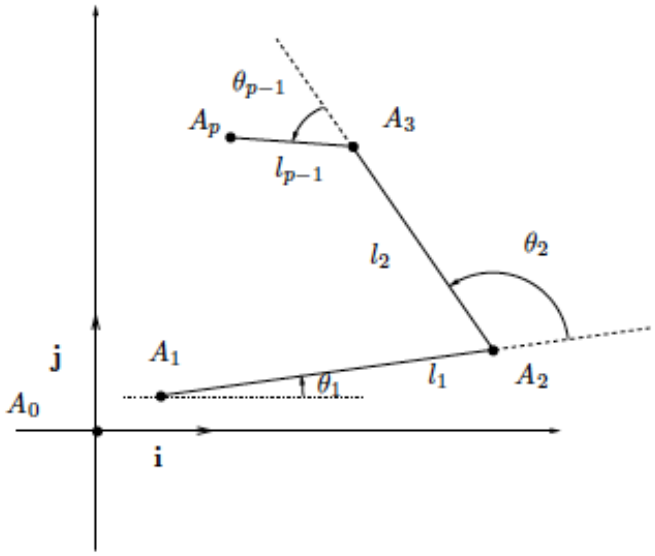

Figure 6. General geometrical representation of the skeletal model

For both tasks, the limbs were modeled as rigid bodies rotating around frictionless hing joints. Given p limbs, the joint positions are defined by the points $A_j(x_j, y_j)$ with $j \in \{1 \dots p\}$ and $p = 3$ and $p = 4$ for pointing task and squat jump respectively. Thus, the position of any joint is given by

$$zA_j = zA_1 + \sum_{n=1}^{j-1} l_n exp\left(i \sum_{k=1}^{n} \theta_k\right) \quad (4.1)$$

Where I is the imaginary unit and zA_1 is the affix of A_1.

4.2 Determination of sigmoid parameters

Sigmoid parameters were obtained from a multi-stage optimization procedure. First, t_b, t_e, θ_b, θ_e, α, β and κ were estimated from experimental data. The scale parameters were defined so that the absolute angular velocity peak occurs between t_b and t_e and its sign changes at the endpoint of this interval. Thus, the shape parameters α, β and κ were determined tanks to (2.6).

First optimization consisted in minimizing the sum of square of differences between experimental angles and those obtained from the sigmoid models at each instant. The optimization was achieved for each sigmoid with the lsqcurvefit function provided in Matlab software. Initial values of parameters were set from estimations of experimental data described previously. This optimization stage will be further referred to as local optimization.

Secondly, differences between experimental and model reconstructed joint positions were minimized in a least square sense. Compared to the previous stage, this optimization can be considered as global since for the latter, the parameters of the sigmoids were determined simultaneously. Computation of model-based joint positions implies the lengths of the limbs to be provided. For the pointing tasks, the optimization was performed using (i) mean experimental limb lengths (semi-global optimization) and (ii) limb lengths as model parameters (global optimization).

4.3 Squat jump specific procedure

The modeling of the jump focused on the position of the joints in a reference frame located at the distal extremity of the foot. Thus, the optimization consisted in fitting the experimental joint positions of ankle, knee, hip and shoulder with the model parameters in this reference frame. Since joints do not remain fully extended after the takeoff, differences were not taken into account during the whole movement. This prevented the model from underestimating the necessary amplitude of joint extensions. Therefore, differences between experimental and model-based data were considered during the intervals corresponding to increase of vertical joint coordinates in the given reference frame (e.g. the error at the ankle joint was only taken into account while the vertical distance between the knee and the foot extremity increased).

Second stage of optimization included non-linear constraints on position, velocity and acceleration of the body CoM computed from sigmoid model. It was imposed that the body CoM position computed from both the sigmoid model and the force plate data were similar at the instant t_1 for which the marker located on the distal extremity of

the foot started to move upward. At this instant, equality for the coordinates of both velocity and acceleration of body CoM obtained from kinetic and kinematic data was also required. Finally, body CoM vertical acceleration was constrained to be greater than -9.81 m.s^{-2} before t_1 ensuring that takeoff occurs necessarily after t_1. From t_1 to the end of the jump, the movement of A_0 was set so that kinetic and kinematic-based movement of the CoM were similar. This results in a continuous characterization of the movement position, velocity and acceleration. It should be noticed that using similar constraints for jerk and further derivatives could have led to description of class C_3 and higher.

4.4 Modeling accuracy

At each instant *i* of the joint *j*, the optimization accuracy can be quantified by the difference between experimental data (x_j^i and y_j^i) and sigmoid-modeled data (X_j^i and Y_j^i):

$$\varepsilon_{i,j} = \sqrt{\left(X_j^i - x_j^i\right)^2 + \left(Y_j^i - y_j^i\right)^2} \quad (4.2)$$

In further analysis, maximal ε_{max} and mean ε_{mean} values of these differences were used to account foir the fitting accuracy of the modeling procedures.

4.5 Statistical analysis

For both maximal and mean accuracies, the Shapiro-Wilk test reported unnormal distributions. Thus, statistical tests were realized on normally distributed $\log_{10}$ of observations (*i.e.* errors and computation time). Firstly, anovas for repeated measures were performed for errors and computation time. When anovas reported significant results, post-hoc tests were performed to check for differences between the sigmoid models and the optimization procedures. All the tests were realized with R and statistical significance was set at 95% confidence level, *i.e.* $p<0.05$.

5. Results

The results were obtained from 304 pointing tasks and 120 squat-jumps. These results are very accurate from numerical viewpoint (Figure 7). Indeed, in pointing task, in 95% of cases, for the three models, ε_{max}, was smaller than 2.894 cm. ε_{mean} was smaller than 0.824 cm. For squat jumps, ε_{max} and ε_{mean} wrer respectively equal to 8.492 cm and 2.882 cm.

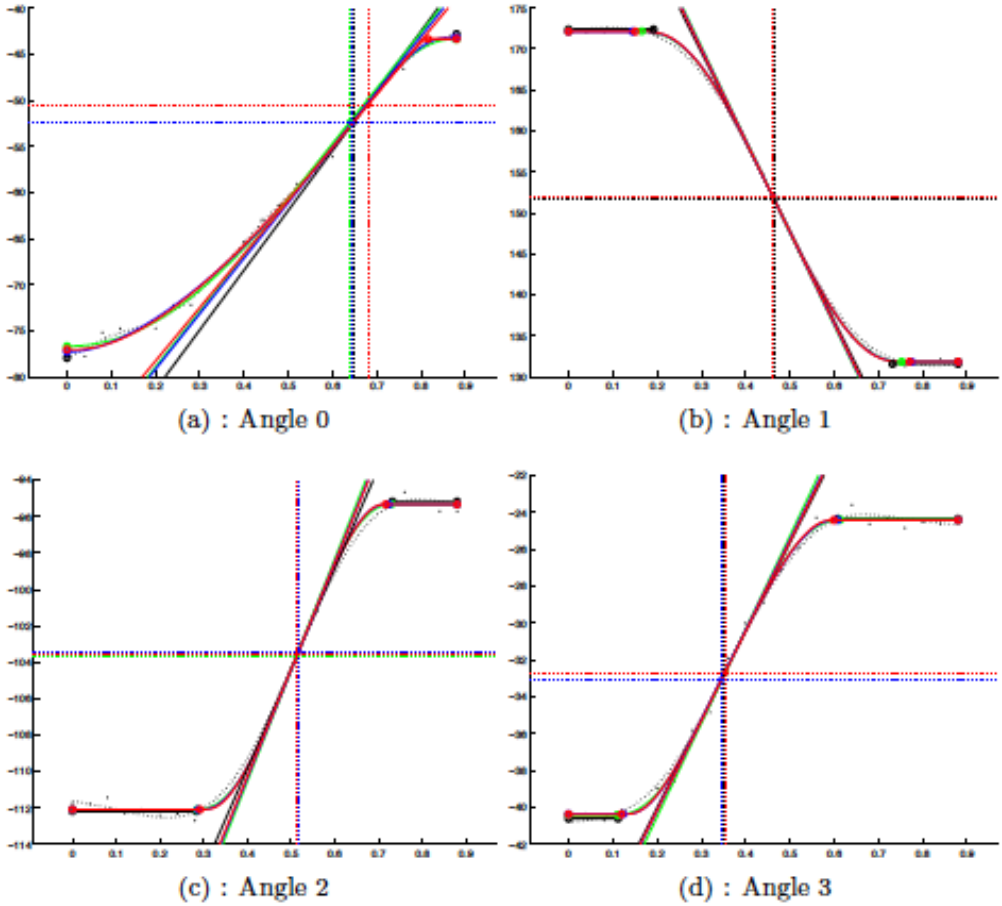

Figure 7. Time histories of joint angles in pointing task. Experimental data are plotted with black points, INVEXP model with red line, NORM model with blue line and SYM model with green line.

6. Discussion

This study evaluated different optimization methods to fit joint trajectories produced during pointing tasks and squat jumps. The evolution of joint angles during the movements was modeled using three sigmoid shaped functions. Assuming a constant length of the limbs, the whole movement was reconstructed from the sigmoid models parameters. For each movement type (i.e. pointing tasks and squat jumps) and sigmoid model, different optimization methods were investigated. In the literature, only Plamondon used a similar approach. However among the published articles, experimental data were presented only in (Plamondon, 1998). Furthermore, no quantitative results were provided and the data was presented for a single subject. This does not allow to compare the present models with Plamondon's one. However, as mentioned earlier, the models used in the present study are defined on a bounded time interval contrarily to the log-normal models for which the end of the movement is not clearly defined.

Differences between original and reconstructed data were lower for pointing tasks than for squat-jumps. The relatively greater amplitude of the joint trajectories could explain this result during the jumping movement. Moreover, the modeling of the skeleton assumes rigid bodies between the joints. Considering the pointing tasks, it can be supposed that the length of the modeled limbs is quite constant. This assumption is supported by the similarity of the errors observed for global and semi-global methods. The rigid bodies assumption would be less true for squat-jump, especially for the trunk limb. Indeed, the spine is composed of many joints which allow bending of the trunk and thus, the trunk may be divided into two segments to ensure that the rigid bodies model is close enough to the reality of the movement.

The modeling methods proposed in this study deal with planar movements. The higher errors obtained with modeling of squat jumps may be explained by the movement of the joints along the transverse axis, especially for the knee. In comparison, pointing tasks would be closer to a real planar movement since the movement is performed on a planar surface.

Concerning optimization methods computing velocity, computation lasted longer for semi-global method than for local one in pointing task. Global optimization executed with similar velocity compared to semi-global method.

Thus, global optimization should be used unless specific purposes are researched. For the squat-jumps, the present results show that unsurprisingly, using the constrained method is much more longer than the unconstrained optimization.

For both pointing tasks and squat jumps, similar accuracy was obtained with the three models of sigmoids. Among the two movements and the optimization methods, it appears that the NORM model allows fastest computation. Considering SYM and INVEXP models, the non-linear equation solving and the numerical integration can explain their relatively slower execution respectively. NORM model formulation takes advantage of the native implementation of the erf function in Matlab software thus ensuring fast computation.

7. Conclusion

The present results show that joint trajectories during planar movements such as pointing tasks or squat-jumps can be modeled using meaningful kinematic parameters. Among the three sigmoid models tested in this study, it appears that the NORM model is computed faster and allows better data fitting of the pointing tasks than other models. On the contrary, for squat-jumps, INVEXP and SYM models fitted better original data. From these results, it can be suggested that INVEXP and NORM models should be used preferentially. Indeed, the INVEXP model did not lead to better results and needs substantial computation time compared to other models. Despite the important computation time, INVEXP model may be useful for modeling specific movements, especially fast movements, which may not allow a good fitting with NORM model due to the relatively small definition domain of this model. For relatively slow and smooth movements, NORM model should be primarily used. Considering the class of the three models, INVEXP or NORM models should be used when the jerk has to be computed, since it can be analytically determined from the models formulation. If the jerk is not considered as a relevant parameter, both velocities and accelerations can be obtained analytically whatever the used model. Furthermore, slow data acquisition rates should not affect much the quality of the fits since only three points are needed to compute the shape parameters of the three models.

References

Bastien, J., Legreneur, P. and Monteil, K. (2010). A geometrical alternative to Jacobian rank deficiency method for planar workspace characterisation. *Mechanism and Machine Theory* **45**, 335-348.

Creveaux, T., Bastien, J., Villars, C. and Legreneur, P. (2012). Model of joint displacement using sigmoid function. Experimental approach for planar pointing task and squat jump. *arXiv preprint arXiv:1207.2627*, 1-28.

Plamondon, R. (1995). A kinematic theory of rapid human movements. *Biological Cybernetics* **72**, 309-320.

Plamondon, R. (1998). A kinematic theory of rapid human movements: Part III. Kinetic outcomes. *Biol Cybern* **78**, 133-145.

Plamondon, R., Feng, C. and Woch, A. (2003). A kinematic theory of rapid human movement. Part IV: a formal mathematical proof and new insights. *Biol Cybern* **89**, 126-138.

Soechting, J. F. and Lacquaniti, F. (1981). Invariant characteristics of a pointing movement in man. *J Neurosci* **1**, 710-720.

van Ingen Schenau, G. J. (1989). From rotation to translation: constraints on multi-joint movements and the unique action of bi-articular muscles. *Human Movement Science* **8**, 301-337.

Winter, D. A. (2009). Biomechanics and motor control of human movement - Fourth Edition. Hoboken, New Jersey: John Wiley & Sons, INC.

Zelaznik, H. N., Schmidt, R. A. and Gielen, S. (1986). Kinematic properties of rapid aimed hand movements. *Journal of motor behavior* **18**, 353-372.